Development of ITER Equatorial EC Launcher

K. Takahashi[1], K. Kajiwara[1], Y. Oda[1], N. Kobayashi[1], K. Sakamoto[1], T. Omori[2] and M. Henderson[2]

[1]Japan Atomic Energy Agency (JAEA), 801-1, Mukoyama, Naka, Ibaraki 311-0193 Japan

[2]ITER Organization, Route de Vinon sur Verdon, 13115 St. Paul lez Durance, France

E-mail contact of main author: takahashi.koji@jaea.go.jp

Abstract. The electron cyclotron (EC) equatorial launcher has successfully passed the preliminary design phase and is advancing toward a final design. In the process, the launcher design is undergoing a series of prototype tests and design enhancements all aimed at improved reliability and functionality of the equatorial launcher. The design enhancements include adaptation of the launcher steering angles such that one of three beam rows of the launcher is necessary flipped to perform counter current drive (to conform to a new ITER physics requirement). Also the top and bottom steering rows have been tilted with angle of 5º in the top and bottom beam row are tilted so that all beams can access from on axis to near mid-radius. A quasi-optical configuration for the in-vessel millimetre (mm)-wave transmission line of the launcher has also been adopted that increases the design reliability and simplifies the manufacturability, which includes a reduction in fabrication cost. Nuclear analysis of the launcher indicates that the launcher has the shield capability to satisfy the dose rate criteria (100μSv/h), however, the dose rate at the launcher back-end can be increased by the influence from the surroundings. High power experiment of the mock-up of the mm-wave launching system confirmed the successful steering capability of 20º~40º. It was found that some of stray RF propagated in the beam duct and behind the mirrors. Prototype tests include the fabrication of mock-ups for the blanket shield modules showed no technological issue on the fabrication and the cooling functionality.

1. Introduction

ITER will install a 170 GHz, 24 MW Electron Cyclotron Heating and Current Drive (EC H&CD) system, which will be used for central heating and current drive applications such as attain steady state and high performance plasma operation, and suppress MHD instabilities such as neoclassical tearing modes and sawteeth. The system consists of twenty-four 170GHz, 1MW gyrotrons [1-3] planned to be installed in the annex building, so-called "RF building". Each gyrotron is connected to a transmission line [4, 5] that directs the power to either an equatorial [6] or four upper launchers [7] that are installed in the respective ports of the vessel. The Japanese Domestic Agency (JA-DA) will procure and supply the Equatorial Launcher (EL) for the ITER organization.

The EL final design and prototype testing has been commissioned to the Japan Atomic Energy Agency (JAEA) for the ITER project. Figure 1 shows the schematic view of the present design of the equatorial launcher. The launcher consists of the shield blanket structure located in the front region facing to plasma and the port plug structure, the later houses the millimeter (mm)-wave components, the neutron shield structure and the cooling water lines. The blanket structure is composed of fourteen blanket shield modules (BSMs) to protect the launcher components from neutrons and thermal radiation from plasma. Three openings are configured in the BSM assembly, which are used to inject the 24 mm-wave

beams from the launcher. The EL BSM surface is recessed 10cm from the surface level of the neighboring wall mounted blankets, which avoids parallel heat flux and limits the thermal loading to < 0.5 MW/m^2.

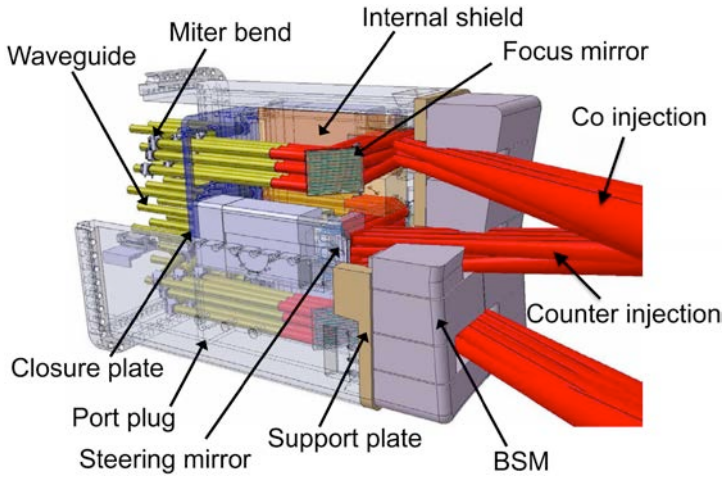

Fig. 1 ITER equatorial EC Launcher. It consists of the shield blanket structure located in the front region facing to plasma and the port plug structure that installs the mm-wave components, the neutron shield structure and the cooling water lines.

The EL presents significant technological challenges that include the transmission of ≥20 MW mm-wave power during long pulse operation (≤3,600 sec), include a rotating mirror capable of injecting (reflecting) up to eight of these beams with toroidal steering capability from 20º to 40º, and compatible with the ITER environment, which includes the thermal and electromagnetic loads and compliant with the nuclear shielding requirement.

The original launcher was designed to inject all 20 MW (24 beams) in the co-ECCD direction (co-linear with the plasma current). However, the design change requests, which introduced two modifications in the steering angles with the aim of enhancing the physics capabilities and/or the range accessible across the plasma cross section, was proposed in 2009. The first of these changes was to inject one-third of the power from the equatorial launcher in the counter-ECCD direction. A balance of co- and counter-ECCD offers the capability to provide pure heating without modifying the current density profile as well as increased flexibility in control of the q-profile. The second modification was to introduce a 5˚ tilt in the beams from the top and bottom row so that all beams can access from on axis to near mid-radius.

2. Equatorial EC launcher design by analysis

The equatorial launcher (EL) groups the 24 mm-wave beams into three sets. Each set assembles eight waveguide lines together and propagate these beams in free space via one fixed and one steering mirror. The power handling requirement of the mm-wave per a line in the equatorial EC launcher has increased from 1 MW to 1.8 MW in prospect of the future power upgrade to 40 MW. In order to meet the requirement, each mm-wave beam expands as it propagates from the waveguide to the first mirror. The beam expansion reduces the peak power density of the mirrors. The two mirrors also form a dog-leg, which helps to reduce direct neutron streaming down the beam path to the waveguide. The steering mirror rotates ±5˚ to provide the ±10º beam rotation in the toroidal direction. Note that the steering mirror has a direct line of sight to the plasma and is subject to additional thermal and nuclear

radiation as well as surface erosion and impurity coating, both of which further increase the mm-wave thermal loading on the mirror.

The optical design of the mirrors is optimized to ensure compliance with the heat loads (1.8 MW/line and plasma radiation), moderate focusing such that the power deposition of the eight beams is roughly 20% of the plasma cross section and ensure that the transmission efficiency of the quasi-optical(QO) region is as high as possible. The optimized optical design uses curved surfaces to providing the greatest flexibility in the optical design for control of the mirror heat loads and beam transmission efficiency. The resulting peak poewr density has been significantly reduced to a tolerable level of $\leq$2.1MW/m^2. This level avoids complicated cooling configurations (such as hypovaportron cooling) thus simplifies manufacturing and reduces fabrication costs. The expected free space beam radius at absorption location in the plasma is 16~22cm and transmission efficiency in the QO region is 98.4~99% as shown in Fig. 2. The transmission efficiency is based on only HE_{11} content of the transmitted beam from the waveguide and an ideal coupling to the TEM_{000} Gaussian mode at the waveguide aperture. The surface roughness of 1.7 and the beryrium coating (several skin depths) on the surface are assumed for the steering mirror.

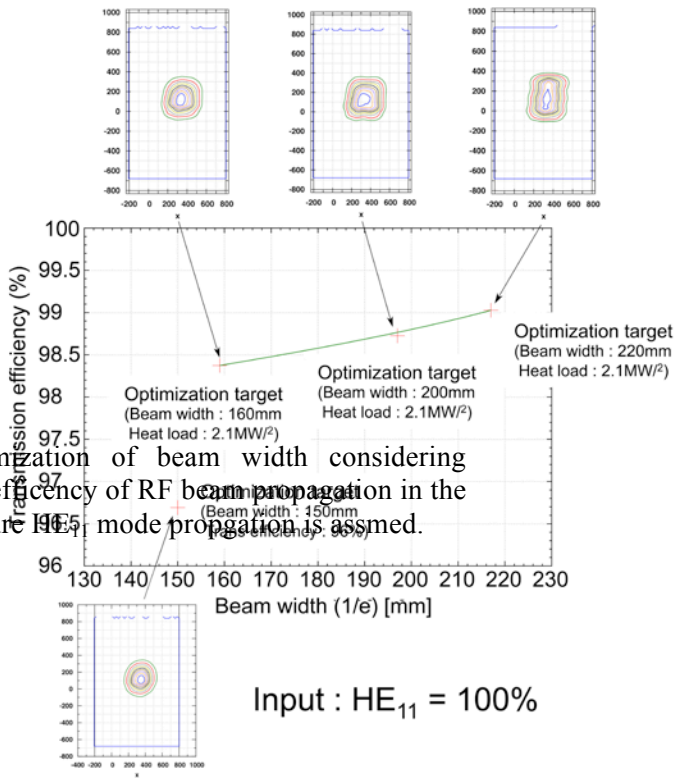

Fig. 2 Optimization of beam width considering transmission efficency of RF beam propagation in the launcher. Pure HE_{11} mode propgation is assmed.

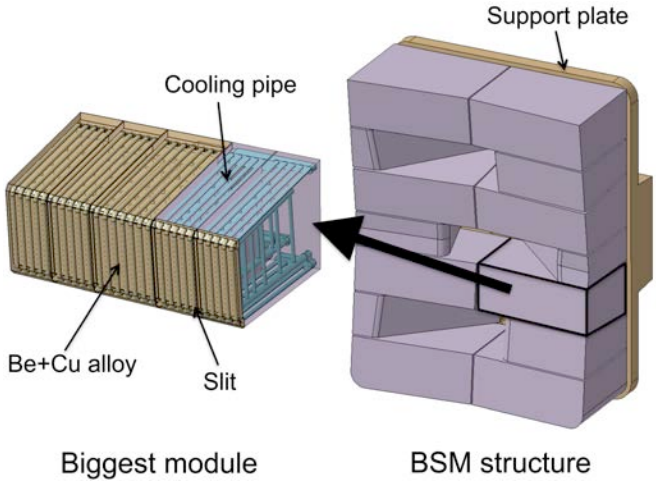

Fig. 3 Blanket for equatorial launcher. Overall structure (right) and biggest module (left). The plasma facing surface has the structure of Be armor and Cu alloy. The vertical slits are introduced to the biggest module.

The blanket shield structure is segmented into 14 modules with the three openings for the transmission of the mm-wave beam set into plasma as shown in Fig.3. The EL blanket shields have a similar functionality as that of the wall mounted blanket and therefore consist of three layer; the Be armor, the Cu alloy heat sink and the nuclear shield body. Both layers of heat sink and shield have several embedded cooling tubes and channels. The EL modules are supported from a single back plate. In order to minimize the eddy current induced by plasma current quench, vertical slits have been introduced in each of the large modules. The resulting electromagnetic (EM) induced torque on these modules is reduced by half and well within the design criteria for the material strength. Thermal hydraulic analysis of the module was also carried out. A maximum calculated temperature was 320 ºC in the shield layer using the designated flow from the Primary Heat Transfer System (circuit used for cooling in-vessel components). The resulting temperature difference and pressure drop were calculated to be 45 ºC and 0.48 MPa for the module assembly, which is well within design requirements.

Nuclear analysis of the equatorial launcher was carried out to determine heat and/or particle loads on its components and also to evaluate the possibility of "hands-on maintainability" (personnel accessibility) to the launcher back-end. A Monte Carlo N-Particle (MCNP) transport code [8] is used for the simulation of neutron transport and one-step MC method [9] is applied for the shut down dose rate to minimize numerical calculation error of decay photon flux. The launcher model is developed by transferring the launcher CATIA model with Monte Carlo Automatic Modeling (MCAM) system [10] developed by ASIPP, China and the launcher MCNP model is inserted into the ITER vacuum vessel model "B-lite" provided by the ITER. A significant radiation leak at the gaps between the port walls and port plug frame of the launcher was revealed. Another significant neutron leakage is through the port wall consisting of only stainless steel but without light isotopes such as water. The shut down dose rates was estimated at the port interspace behind the launcher at the same level of the required value of 100 μSv/h. This analysis offers the potential to modify the launchers shielding layout to minimize the above leakage and further reduce the shut down dose rates in the regions of personnel

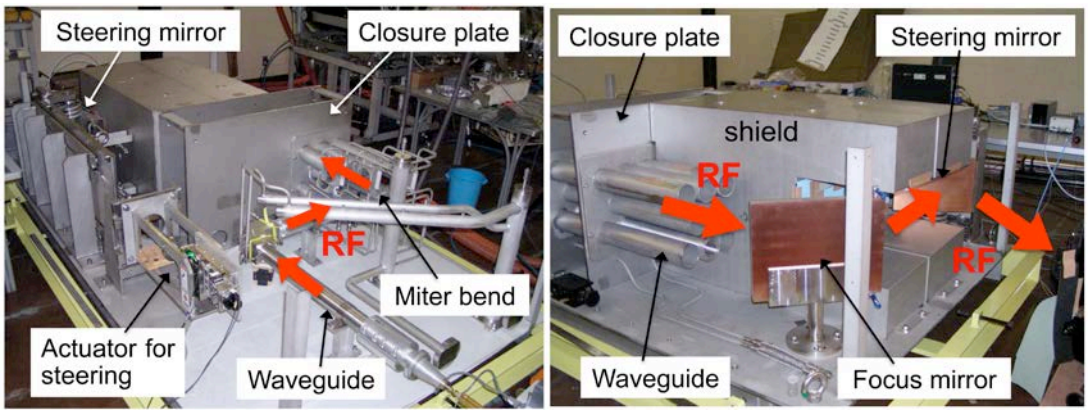

Fig. 4 EL full scale mock-up. Left : rear side, Right : front side. One of three mm-wave transmission sets were fabricated. One of eight waveguide lines can be used for the mm-wave transmission experiment.

3. Fabrication of the launcher mock-ups and testing

The EL full-scale mock-up (Fig. 4) was fabricated based on the design to investigate the mm-wave propagation properties in the launcher, the manufacturability, the cooling line management, how to assemble the components, etc. The mock-up simulates one of three

mm-wave transmission sets. The mm-wave line consists of the steering and focusing mirror and eight dog-legged waveguide lines. Only one of the eight lines can be used to transmit mm-wave power through the launcher. The remaining seven lines are dummy lines, which are used to demonstrate how to assemble the complicated structure of the waveguide components and the cooling pipes.

The EL mock-up was connected to the ITER compatible transmission line and the 170 GHz gyrotron so that high power transmission through the launcher mock-up could be performed. Fig.5 shows the radiated pattern of the beam at both mirrors and at a distance of 2.5m away from the EL mock-up (roughly the distance to the resonance location in the plasma). The steering capability of 20º~40º was successfully confirmed. It was also revealed that the radiated profile at steering mirror agreed with the calculated profile, while the beam propagating after the of the focusing mirror deviated slightly from the calculated shape. This result suggests that some unwanted modes are included in the radiated beam. Transmission of 0.5MW-0.4sec and of 0.16MW-10sec were also demonstrated. The drive mechanism for the steering mirror was also tested and the cyclic movement of 3 x 10^5 was performed with sweep speed of 20º/3sec and angle resolution of 0.03º, compliant with the general objectives of the steering mechanism.

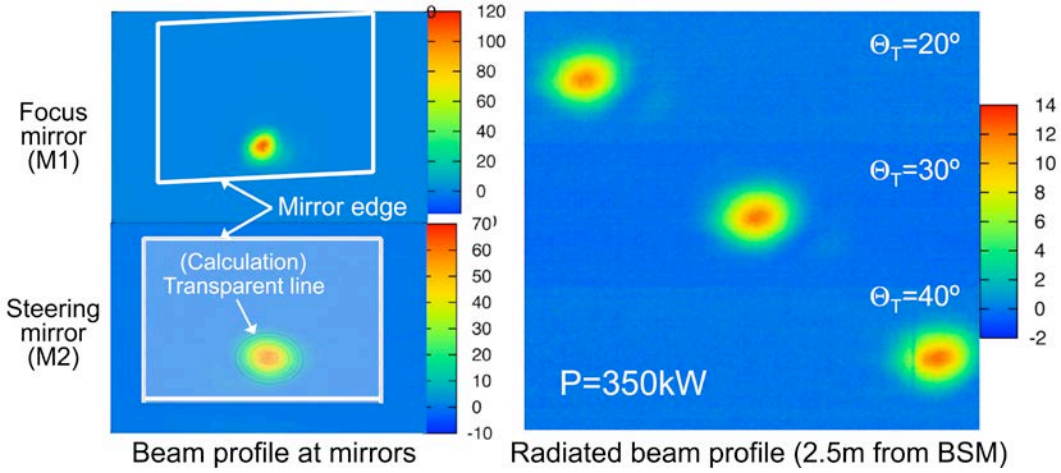

Fig5. Radiated pattern of RF beam power at both focus and steering mirror (left) and the location of 2.5m away from the EL mock-up (right)

The calculated transmission efficiency (>98%) assumed an ideal HE_{11} mode from the waveguide. However, the HE_{11} mode purity as low as 90~95 % could occur at the launcher input due to waveguide sagging, misalignments and mitre bends. Thus, some non-negligible amount of higher order modes will exist at the launcher entry and these modes may be radiated from the waveguide with some radiation angle and randomly scattered in the launcher. This can cause anomalous heating in the launcher components, which are poorly cooled, and may lead over heating and potentially melting of critical components. In addition, the non-HE_{11} modes will modify the beam trajectory through the quasi-optical part of the launcher, resulting in a variation from the measured and calculated beam, as evidenced in the above measurements performed after the steering mirror.

In order to investigate how the scattered mm-wave power leaves the waveguide, an artificial beam duct was inserted along the quasi-optical beam path. The beam duct was made of graphite sheet with thickness of 1mm with the expectation of the scattered power to be partially absorbed in the lossy material. An IR camera was positioned to monitor the temperature rise on the beam duct. Figure 6 shows one example of results. A significant increase in temperature was observed in the wall around the mirrors and the waveguide outlet.

A moderate increase in temperature was observed in the side walls of the duct. This result indicates that multipath reflection of stray mm-waves occurs between the structures in the beam ducts. It is also presumed that some of stray RF can propagate behind the mirrors or toward the location that is poorly cooled.

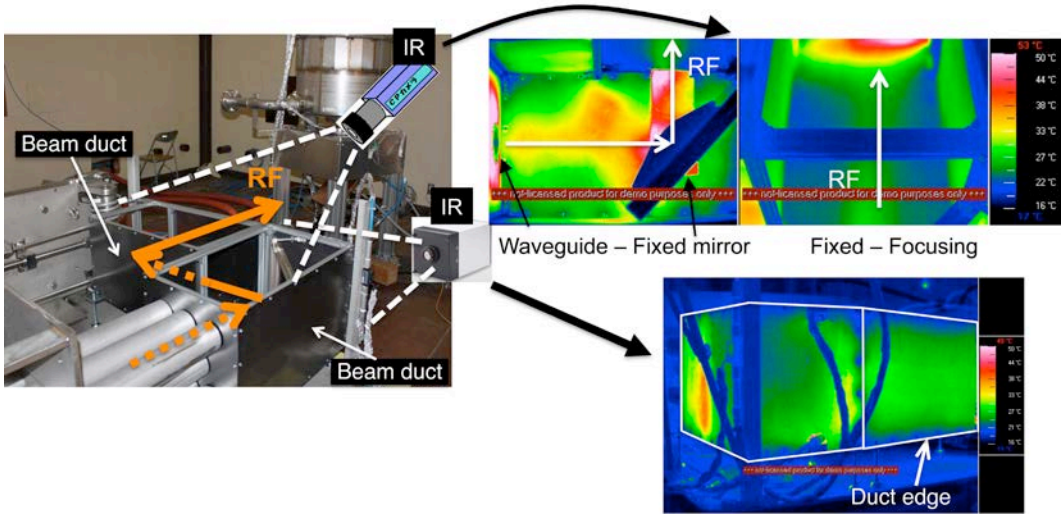

Fig. 6 Temperature distribution of beam duct made of graphite sheet. Top of thermal view were temperature of the bottom and side walls. Bottom shows temperature of the side wall taken from the out side.

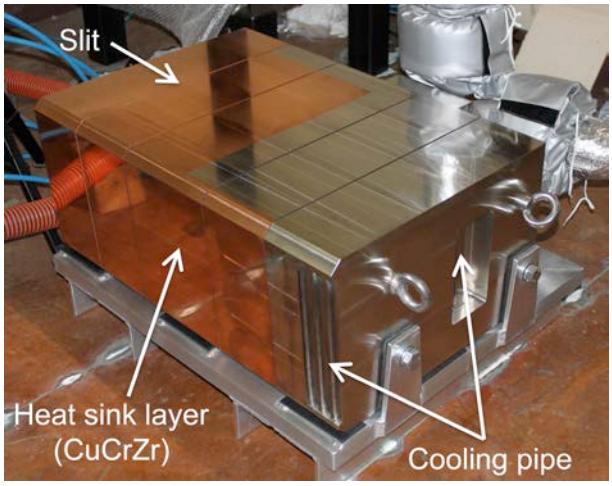

Fig. 7 BSM mock-up. There are several slits to minimize the eddy currents on the module. It has the bare cooling pipess in the first wall (heat sink) and shield layer.

The mock-up of the BSM was fabricated based on the design shown in Fig. 3. The Be armour is omitted due to the lack of handling capabilities of Be in the JAEA lab. However, the heat treatment process of the joint between the Be armour and the Cu alloy (CuCrZr) heat sink layer was carried out. The hot isostatic pressing (HIP) technique was applied for the joint. The joint between the heat sink layer and the shield layer made of stainless steel 316L including the embedded stainless steel tubes was also implemented by HIP. Four 2mm slits are machined vertically into the BSM (to limit the induced EM currents described above). Figure 7 shows the photogaph of the BSM mock-up. It includes cooling pipes located in the heat sink layer and the shield layer as shown in Fig. 7, which permits the monitoring of the coolant flow using an ultra-sonic flow meter. It was preliminary obtained that the measure

water flow was 20% lower than that calculated. The reason of the difference is not determined. Possible reasons include bubbles in the coolant channel or variations in the cooling water temperature, either of which could impact the precision of the ultra-sonic flow meter.

4. Next step

It is important to know how much stray RF power possibly exists in the beam duct and behind the mirror, quantitatively. A calorimetric measurement of the beam duct will be carried out and the result will be used for the final design of the internal shield structures since the beam duct is formed by them. ITER will be proposing the modification of the EL functionality such that the steering direction changes from toroidal to poloidal. This change can provide higher efficiency of driven current beyond $\rho_t \geq 0.4$ although it is not the original design requirement of the EL. On the other hand, this change will have somewhat large impact on the design of the BSM structure and the steering mechanism for the rotatable mirror. Another upcoming design change request is to remove Be armour from the BSM. This is associated with the 10cm-resession of BSM surface from the original position. It will advantage in reduction of the fabrication cost and other material for the armour will have to be considered in stead. The future activities on the EL design and R&D toward the final design will include these technical changes.

5. Conclusion

The electron cyclotron (EC) equatorial launcher has been designed with the adaptation of the design change request of the ITER physics requirement to perform drive counter current and to access all beams from on axis to near mid-radius. The present launcher design adopted a quasi-optical configuration for the in-vessel mm-wave transmission line has the advantage in minimizing the heat load on the mirrors. The design also has the significant impact to increase the manufacturability and design reliability. Nuclear analysis of the launcher was carried out with present of the ITER vacuum vessel model (B-lite). It can be concluded that the launcher has the shield capability to satisfy the dose rate criteria (100μSv/h), however, the dose rate at the launcher back-end can be increased by the influence from the surroundings. The based on the design, the mock-up of the mm-wave launching system and the subcomponents such as the blanket shield module are fabricated to investigate the design availability. High power experiment of the mock-up confirmed the successful steering capability of 20º~40º. Temperature measurement of the artificial beam duct indicates that multipath reflection of stray mm-waves or the side rob of beams occurs in the beam ducts. It is also presumed that some of stray RF can propagate behind the mirrors or toward the location that is poorly cooled. The BSM mock-up was fabricated based on the design to investigate if the design and the expected fabrication technique are feasible. No technological issue on the fabrication was obtained.

6. Reference

[1] K. Sakamoto, A. Kasugai, K. Takahashi et al., Achievement of robust high-efficiency 1MW oscillation in the hard-self-excitation region by a 170GHz continuous-wave gyrotron, Nature Phys. 3 (2007) 411

[2] A. Litvak, G. Denisov et al., Development in Russia of megawatt power gyrotrn for fusion, J. Infrared and MM and Terahelz waves, 32 (2911) 274

[3] J.P. Hogge, T. Goodman, S. Alberti, et al., , First Experimental Results from the European Union 2-MW Coaxial Cavity ITER Gyrotron Prototype, Fusion Sci. Tech., 55 (2009) 204.

[4] F. Gandini, T. S. Bigelow et al., The EC H&CD transmission line for ITER , Fusion Sci. Tech, 59 (2011) 709

[5] K. Takahashi, K. Kajiwara, Y. Oda et al., The EC H&CD Transmission line for ITER, Rev. Sci. Instrum., 82 (2011) 063506

[6] K. Takahashi. K. Kajiwara, N. Kobayashi et al., Improved design of an ITER equatorial EC launcher, Nucl. Fusion, 48, N5 (2008) 054014

[7] M. Henderson, R. Heidinger, D. Strauss et al., Overview of the ITER EC upper launcher, Nucl. Fusion, 48, N5 (2008) 054013

[8] MCNP TM, A General Monte Carlo N-Particle Transport Code,in: J. Briesmeister (Ed.), Los Alamos National Laboratory, Los Alamos, New Mexico, LA-13709-M, 2000.

[9] H.Iida, D. Valenza, R. Plenteda, R. T. Santoro and J. Dietz "Radiation Shielding for ITER to allow for Hands-on Maintenance inside the Cryostat", J. of Nuclear Science and Technology, Supplement 1 (2000) 235-242.

[10] Y. Wu, FDS Team, "CAD-based interface programs for fusion neutron transport simulation," Fusion Eng. Des., 84, 1987 (2009).